Geophysical Research Letters

Key Points:
- Effective radius of *Sargassum* rafts, needed for modeling inertial effects, is calculated from remote sensing by an inverse method
- Including inertia in particle-tracking models results in more *Sargassum* entrainment in eddies and changes in *Sargassum* distribution
- These inertial effects yield increased *Sargassum* in the Gulf of Mexico and Caribbean and loss from the subtropical gyre

Supporting Information:
- Supporting Information S1

Correspondence to:
M. T. Brooks,
mbrooks@umces.edu

Inertia Influences Pelagic *Sargassum* Advection and Distribution

Maureen T. Brooks[1] (ID), **Victoria J. Coles**[1] (ID), and **William C. Coles**[2]

[1]Horn Point Laboratory, University of Maryland Center for Environmental Science, Cambridge, MD, USA, [2]Division of Fish and Wildlife, United States Virgin Islands, USA

Abstract The effect of inertia (resistance to a change in velocity of buoyant finite-sized objects) on the advection of pelagic *Sargassum*, a macroalgae, is a function of the size and density of natural *Sargassum* rafts. Here we present observations of *Sargassum* density and an approach for estimating an effective radius of *Sargassum* rafts from remote-sensing observations. This allows the existing theoretical framework for Lagrangian modeling of inertial effects on spherical particles to be applied to *Sargassum*. Accounting for inertia yields up to a 20% increase in *Sargassum* export from the Sargasso Sea southward and provides a return pathway to the tropics that may be important to maintaining a self-sustaining population. Resolving inertial effects also leads to increases in retention in the Gulf of Mexico and Caribbean Sea, where *Sargassum* inundation events are increasingly common. Including inertial effects in models of *Sargassum* advection could improve predictions of these events.

Plain Language Summary *Sargassum* seaweed has been washing up on beaches in the tropical Atlantic more frequently and in greater volume in recent years. Few measurements have been made of the physical properties of *Sargassum* that would allow more accurate modeling and prediction of these events. In this study, the size, weight, and shape of *Sargassum* rafts are calculated from both field measurements and satellite observations. These properties are then applied to a model of *Sargassum* transport in the Atlantic, where they cause more *Sargassum* to enter and then remain in the Caribbean and Gulf of Mexico. This suggests forecast models of *Sargassum* washup events should include these effects.

1. Introduction

Pelagic macroalgae of the species *Sargassum fluitans* and *Sargassum natans* have been washing up on beaches in the Caribbean, Gulf of Mexico, and western Africa in events of increasing severity and frequency in recent years (Franks et al., 2011; Langin, 2018; Smetacek & Zingone, 2013). This suggests changes have occurred either in *Sargassum* biomass or its distribution due to surface currents. Because *Sargassum* spends its entire life cycle floating at the ocean surface, it is important to understand how it interacts with ocean currents in order to predict its dispersal and locations of potential landfall.

The *Sargassum* biomass in the Gulf of Mexico and tropical Atlantic exerts a strong influence over basin-wide *Sargassum* distribution (Brooks et al., 2018). Previous studies (Brooks et al., 2018; Franks et al., 2016; Putman et al., 2018) simulating *Sargassum* with Lagrangian particles showed potential pathways for *Sargassum* dispersal and highlighted the link between *Sargassum* biomass in the tropical Atlantic and the Caribbean Sea. However, these previous models of *Sargassum* drift fail to account for changes in trajectory caused by the size and mass of the floating rafts.

The finite-size radius and density of a Lagrangian object, like *Sargassum*, dispersing in ocean currents can influence its trajectory through inertial forces (Maxey & Riley, 1983; see also Beron-Vera et al., 2015; Haller & Sapsis, 2008). Inertia, or an object's resistance to changes in velocity, is dependent on the physical properties of the object. Differences in density create inertia between Lagrangian particles and the surrounding water and can cause particles to cross material lines and become entrained in, or expelled from, eddies (Beron-Vera et al., 2015). For buoyant *Sargassum* in the tropical North Atlantic, inertial effects should lead to entrainment in cyclonic eddies and expulsion from anticyclonic eddies.

Differences in entrainment in mesoscale eddies have the potential to impact *Sargassum* dispersal. Eddies in weak background flow propagate westward, with cyclonic eddies tending poleward and anticyclonic tending equatorward (Early et al., 2011; Morrow et al., 2004). Thus, entrainment into a cyclonic eddy will increase
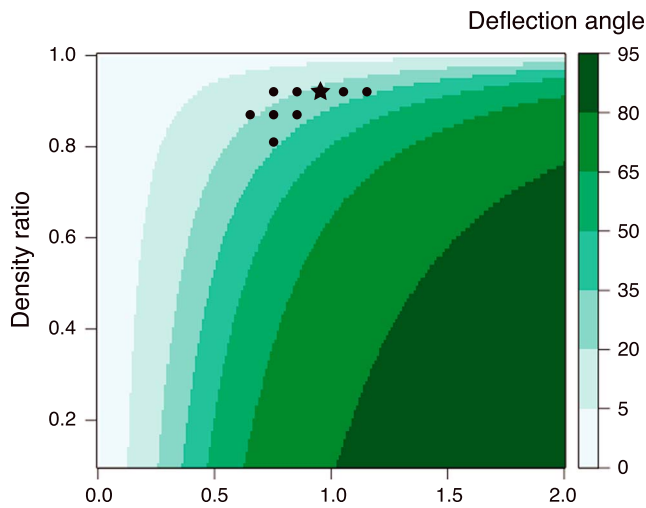
Figure 1. Deflection angle derived from inertial equations for buoyant objects with constant velocity at 10°N. Density ratio is the density of the object divided by that of the ambient seawater. Plotted symbols indicate where model and observed deflection angle distributions were not significantly different for a threshold of $p = 0.01$. The star indicates the effective radius and density ratio of *Sargassum* as determined in this study.

the tendency of *Sargassum* rafts to drift northwest in the North Atlantic. Inertial effects are important for correctly modeling these advective responses because inertia may explicitly alter the likelihood of *Sargassum* crossing an eddy boundary (Beron-Vera et al., 2015; Cartwright et al., 2010).

Modeling inertial effects on *Sargassum* advection requires estimates of both raft density and radius. While density can be measured directly, radius is difficult to determine because *Sargassum* rafts are highly non-spherical. The high abundance of *Sargassum* in the Caribbean in 2018 provided a unique opportunity to apply a novel approach to estimating raft radius. In this study, we calculate the density of *Sargassum* from field measurements and estimate radius using an inverse approach based on comparing the difference between satellite observations of *Sargassum* and of flow streamlines. We then use the density and effective radius to simulate inertial effects on *Sargassum* rafts in the Atlantic to determine the impact on the basin-wide *Sargassum* distribution.

2. Materials and Methods

2.1. Deflection Angle Definition

We defined the *Sargassum* deflection angle as the angle formed between a fluid trajectory and the *Sargassum* trajectory. Angles that corresponded to the theory for buoyant particles, where the inertial particle deflected to the left of the direction of the flow, were assigned positive values. Those to the right were assigned negative values. This angle is an estimate of the difference between the observed trajectory of a finite-sized buoyant object and that of a water parcel with no finite size and a density identical to the surrounding water.

We considered the influence of inertia using the theory for a spherical particle (Maxey & Riley, 1983) as applied to large-scale ocean flow by Beron-Vera et al. (2015). Inertia is a function of radius (r), latitude, and the ratio of the density of ambient seawater (ρ) to the particle density (ρ^P). For a background flow of velocity v, this inertial component is calculated as

$$\tau(\delta-1)fv^{\perp} \tag{1}$$

with

$$\tau = \frac{2r^2}{9\nu\delta} \quad , \quad \delta = \frac{\rho}{\rho^P}, \tag{2}$$

where ν is the kinematic viscosity, f is the Coriolis parameter, and $\perp$ indicates a 90° rotation anticlockwise.

Predicted deflection angle can be calculated using this equation and assuming a constant velocity (Figure 1). Objects with larger radii or with densities that are differ significantly from ambient water will show the greatest deflection. If the effective radius of *Sargassum* rafts is close to that of an individual plant, then radius alone largely determines the strength of inertial effects. However, if it is larger as a result of aggregation, then both density and effective radius control the strength of the inertial effects.

2.2. Density Measurements

Samples of *Sargassum* of at least two different morphotypes were collected from Saint Croix, U.S. Virgin Islands, to determine the density of the macroalgae. Ten samples were retrieved at each of four locations, Robin Bay and Turner Hole on the south side of the island, and Christiansted Harbor and Hibiscus Beach on the north (Table S1 in the supporting information). *Sargassum* was collected by hand in nearshore water of 1- to 2-m depth. Attached flora and fauna were left intact, but free-living organisms and loosely associated vegetable matter were gently removed. The samples were transferred to plastic storage bins containing ambient water for transport. *Sargassum* density was measured within 3 hr of collection. Because less buoyant,
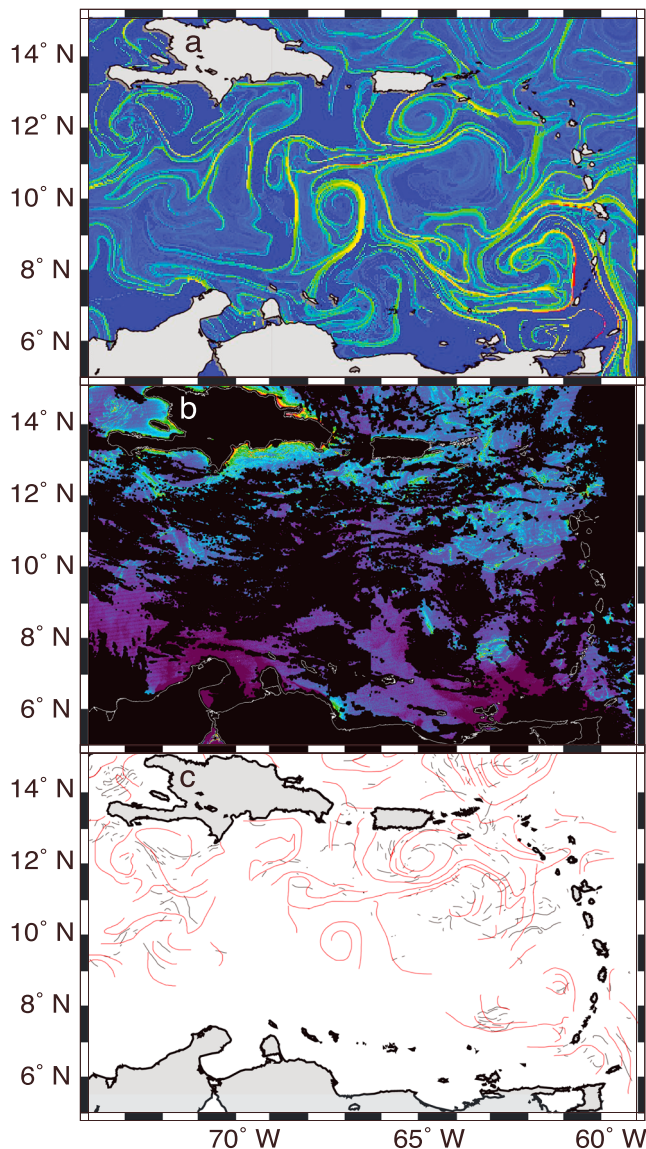
Figure 2. Deflection angle measurement of observations. The (a) finite-size Lyapunov exponent field and (b) Alternative Floating Algae Index (courtesy of the *Sargassum* watch system) were independently traced. (c) Measurements of deflection angle were made where lines of finite-size Lyapunov exponent (red) and *Sargassum* (black) approached each other near underlying circulation features.

subsurface *Sargassum* will not be clearly detected by remote sensing, samples showing signs of decay, or loss of structural integrity, were excluded from this analysis.

A volume of freshwater was added to a graduated cylinder, and the volume and mass were recorded. The subsample of *Sargassum* was blotted dry and weighed on a CAS SW-1W electronic balance. This sample was added to the graduated cylinder. A large steel washer (52-mm diameter, 8 ml, 45 g) was placed on the top of the *Sargassum* to ensure the entire sample was submerged, and the cylinder was reweighed. Mass and volume were recorded, and the density ratio between seawater and *Sargassum* was calculated from wet mass and volume of the *Sargassum* samples.

2.3. Satellite Observations

U.S. National Aeronautics and Space Administration Visible Infrared Imager Radiometer Suite satellite observations (Ocean Color, 2018) from 2018 were selected for analysis. Images of Alternative Floating Algae Index (AFAI; Hu, 2009; Wang & Hu, 2018; Wang et al., 2018) in the Western Tropical Atlantic, Caribbean, and Gulf of Mexico in March–July 2018 were examined to locate putative *Sargassum* aggregations (SaWS, 2018). These were referenced against the finite-size Lyapunov exponent (FSLE) field derived from satellite altimetry (AVISO, 2018; d'Ovidio et al., 2004) to find co-occurrences of *Sargassum* with coherent eddies. FSLE contours and AFAI local maxima were independently traced by hand using a Huion 1060PLUS digitizing tablet and Photoshop software (Adobe Photoshop CS5 v12.1, Adobe Systems, 2011).

The FSLE field and AFAI for the same date and location were subsequently overlaid and examined. Where eddies and *Sargassum* co-occurred in space and time, the angle of orientation of lines of *Sargassum* and the nearest FSLE contour were measured, and the deflection angle was calculated by difference (Figure 2). This assumes that the AFAI line reflects the orientation of the *Sargassum* advection. A 20-km guide ruler was used for consistent measurements and to provide a minimum scale below which *Sargassum* aggregations were not considered. A total of 91 *Sargassum* lines were measured from four dates with clear images and high regional *Sargassum* abundance, 28 and 30 May 2018 and 7 and 15 June 2018. Probability density functions and comparison with model results using the Anderson-Darling k-sample test were calculated using R (R Core Team, 2018).

2.4. Modeling

Daily output from a data-assimilating Hybrid Coordinate Ocean Model (HYCOM.org GLBa0.08 experiment 91.2) simulation at 1/12° resolution (Chassignet et al., 2009) was used as input for an off-line Lagrangian particle advection model (Garraffo et al., 2001). The study region extended from 15°S to 65°N and from 100°W to 20°E. A tropical subregion from 5°S to 25°N and from 90°W to 35°E was used for validation with satellite observations, and the full study region was used in subsequent analyses of *Sargassum* dispersal. Code for buoyant *Sargassum* particles (Brooks et al., 2018) was updated to include inertial forces as a function of particle density and effective radius (Beron-Vera et al., 2015). The source code is available at the GitHub Inc. website (https://github.com/mtbrooks/inertial-particles).

To determine the temporal scope most appropriate for comparison with the satellite observations, the displacement from initial position for 7,300 noninertial particles initialized on a 0.5° grid within the tropical subregion for 30 days was measured at daily intervals. A duration of 8 days was chosen for subsequent

experiments because more than 98% of particles that did not go aground had reached a minimum displacement of 20 km in 8 days. Note that 20 km was used as the minimum distance for the angle of deflection calculations derived from satellites.

Model sensitivity to particle radius and density was explored to determine best fit to the satellite-derived deflection angle distribution. Particle density was constrained to within $\pm12\%$ of the field measurements (consistent with the range in variability of those measurements), while radius was varied between 0.05 m (the approximate size of a single *Sargassum* plant) and 2 m. Particles were initialized 8 days prior to the date of the each of the satellite images, so the model and satellite observations could be compared at the same date. All particles that had traveled at least 20 km from their initial position were used in subsequent calculations.

Deflection angle between inertial and noninertial particles was calculated as the angle between the lines connecting the initial position and the noninertial end point, and the initial position and the inertial end point. As in the satellite analysis, angles where the inertial particle deflected to the left of the direction of the flow were assigned positive values; those to the right were assigned negative values. The ensemble distribution of each angle was compared with the results of the satellite analysis above to inversely estimate effective *Sargassum* raft radius.

A connectivity model experiment examined the effect of inertia on the *Sargassum* distribution throughout its range. A total of 51,100 noninertial particles (number determined based on the analysis in Brooks et al., 2018) were initialized randomly throughout the full study region. These particles were launched daily over 1 year, and each particle was tracked for 1 year. The study region was divided into 14 subregions based on the local circulation and importance to the *Sargassum* seasonal distribution, and connectivity between each pair of regions was calculated. The simulation was then repeated for particles with inertial characteristics best matching the observed radius and density of *Sargassum*, and the difference between the noninertial and inertial particle distributions was evaluated.

3. Results

3.1. *Sargassum* Density

The density of *Sargassum* was variable, ranging from 0.45 g/ml (at Robin Bay) to 2.50 g/ml (at Turner Hole). Density was consistently high at the Turner Hole site, with six out of 10 samples being denser than the ambient water. This may be due to the age of the *Sargassum* at the location, or the smaller size of the fragments there. The mean *Sargassum* density from all samples was 1.04 g/ml (standard deviation of 0.38 g/ml), unexpectedly high for buoyant, healthy biomass. The highest variability was in the smallest samples, which did not always have a consistent ratio of buoyant pneumatocysts to biomass compared with the larger samples. Excluding those samples with a mass of 15 g or less reduced the standard deviation of the mean from 0.34 to 0.12 g/ml and resulted in a mean density of 0.94 g/ml. The ratio of *Sargassum* density to that of ambient water for this subset of samples was 0.92.

3.2. Satellite Observations

Observed deflection angles ranged from $-92.1°$ to $110.7°$, with a mean of $5.6°$ (Figure 3a). The distribution of deflection angles is skewed positive with a peak frequency between $12.5°$ and $17.5°$. While an idealized distribution of deflection angles due only to buoyant particles experiencing inertia should be entirely positive, other factors such as temporal variability in velocity fields that formed *Sargassum* lines, submesocale processes unresolved by the altimetry, and windage are present in these observations leading to variability in deflection angle. Given that the prevailing winds in the Caribbean blow from east to west, the effect of windage on deflection angle should result in slightly larger angles on the east side of cyclonic eddies and the west side of anticyclonic eddies, where wind and inertia are acting in the same direction, and slightly smaller angles on the corresponding opposite sides. An Anderson-Darling k-sample test found small but significant ($p < 0.05$) differences between the angle distributions of these two groups in our observations, with *Sargassum* on the east side of cyclonic eddies and west side of anticyclonic eddies having a peak at a deflection angle of $21°$ and *Sargassum* in the opposite group having a peak frequency at $10°$. Beron-Vera et al. (2016) extended the theory for inertial particles to include windage on a spherical float; however, application
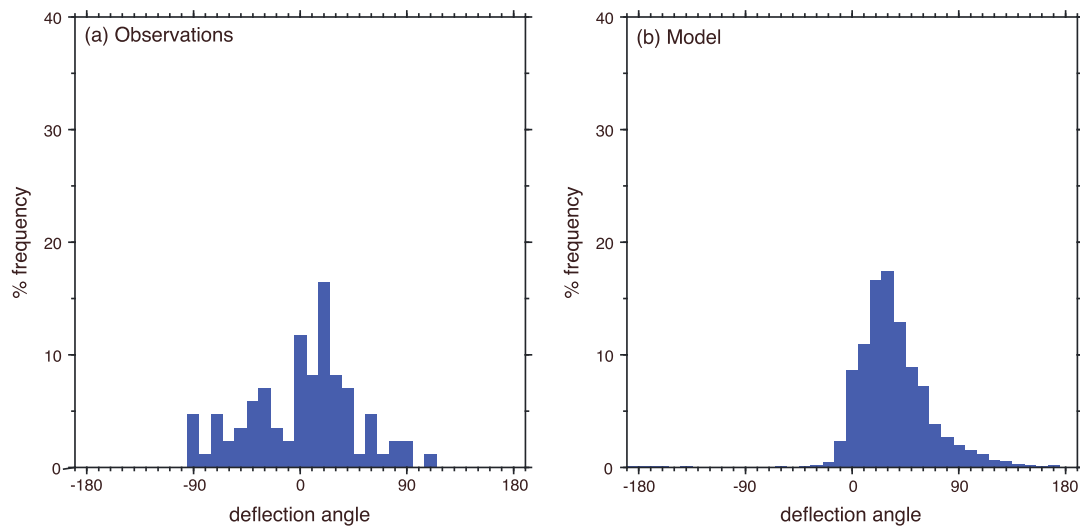
Figure 3. Histograms of (a) observed and (b) modeled deflection angle, used to estimate *Sargassum* effective radius.

of windage effects to the complex morphology and predominantly submerged *Sargassum* rafts remains a challenge.

3.3. Model Validation

Deflection angles in the sensitivity study model simulations were skewed positive, with much less variance than the observations (e.g., Figure 3b). This is as expected, as the model does not resolve submesoscale processes, all particles have the same radius, and we did not include the effects of windage. The probability density functions of the distribution of angles for both model experiments and observations were calculated, and the positive distributions were compared using the Anderson-Darling k-sample test. Particles with effective radii less than 0.65 m or greater than 1.15 m had deflection angle distributions that were significantly different from the observed *Sargassum* (p values < 0.01). The simulation with a density ratio of 0.92 and effective radius of 0.95 m had a peak frequency that most closely matched that of the observations, and these values were selected for the *Sargassum* distribution experiment.

3.4. Inertial Effects on *Sargassum* Distribution

Although *Sargassum* has a density very close to seawater and a relatively modest effective radius, connectivity analysis shows that the cumulative effects of inertial deflection can alter its basin-wide distribution (Figure 4; seasonal pattern in the supporting information). These differences reflect changes in *Sargassum* entrainment in eddies. Over the course of the experiment, 61% of inertial *Sargassum* became entrained in an eddy-like structure, as defined by having >180° of particle trajectory rotation in a 5-day period. This is a fivefold increase from the noninertial simulation, which had only 12% entrainment.

Inertial particles are 48% more likely to be retained in the Western Gulf of Mexico (region 1) at timescales of 90 days and longer (Figure 4, diagonal elements). The Caribbean (region 3) also retains 36% more *Sargassum* in the inertia experiment, while also experiencing a small annual increase in particles entering from the northern tropics (region 7). There are large seasonal differences in the exchange between the equatorial region (region 10) and the northern tropics (region 7), matching the timing of the North Brazil Current retroflection.

Inertial effects also alter the *Sargassum* distribution in the subtropical gyre. The northern Sargasso Sea (region 8) retains less *Sargassum* when inertia is considered, though there is more accumulation along the southern boundary (region 7). Western Atlantic regions 4 and 5 export less *Sargassum* eastward into the central gyre (region 8) when inertial effects are accounted for. At the northeast extent of *Sargassum*'s range (region 12) annual mean connectivity and retention showed only decreases in the inertia experiment, due to the rafts grounding or exiting the domain more frequently. Along the coast of western Africa in a region of high divergence in the circulation due to upwelling (region 11), there is an equatorward shift in
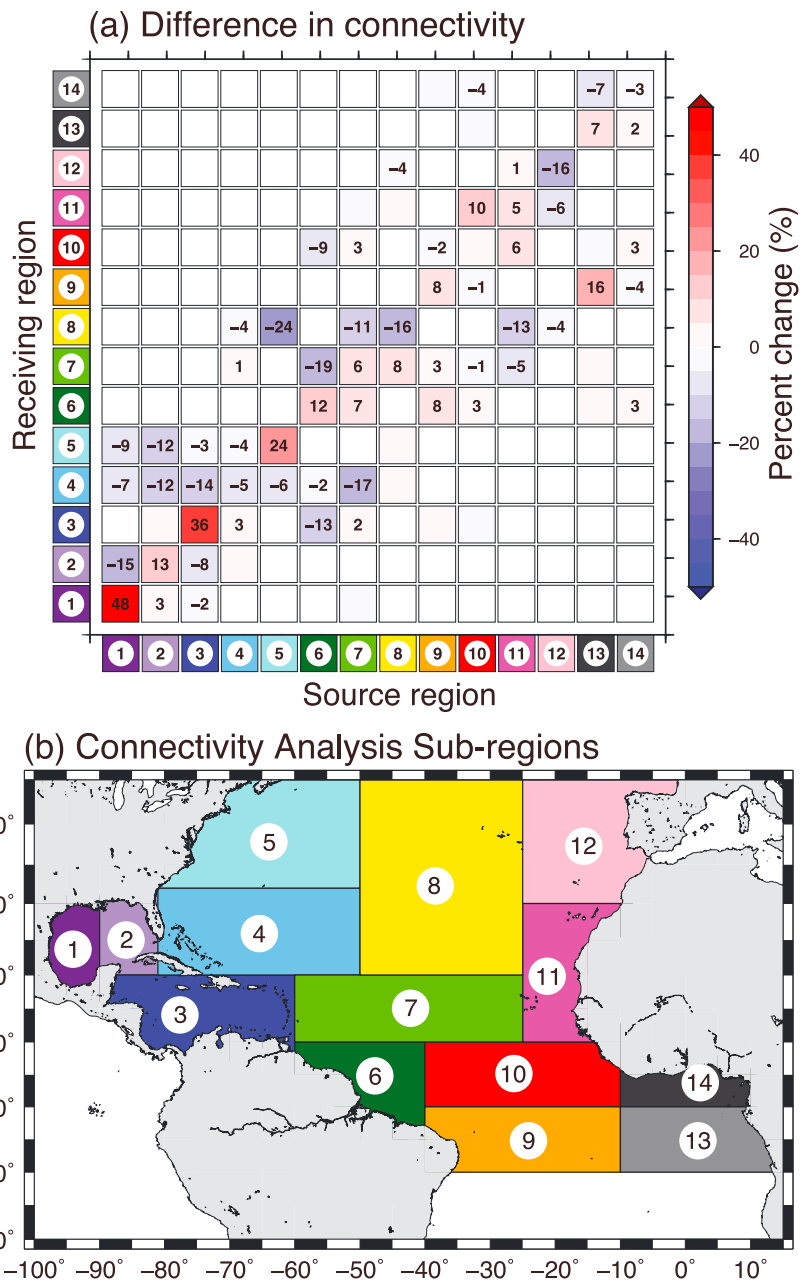
Figure 4. Effect of inertia on *Sargassum* trajectories and distribution throughout its range. (a) Changes in connectivity between regions when inertia is considered. Values are shown for changes of 1% or greater. (b) Subregions of the model domain used in this analysis.

connectivity, away from the central gyre. Additionally, there is a seasonally varying increase in *Sargassum* escaping the gyre to the south (region 7), with an annual mean of 8% and a peak of nearly 20% in November. Broadly, all source regions south of 20°N exported less *Sargassum* to the Sargasso Sea when inertia was accounted for.

There were also changes in connectivity for regions south of the equator. Inertial rafts were more likely to be retained locally (regions 9 and 13), although there was a slight increase in export from the western side of the basin northward across the equator to the region of the Amazon River plume (region 6). A seasonal 5% increase in connectivity with the northern tropics was also found for *Sargassum* that originated south of the equator in the spring.

4. Discussion and Conclusions

The density of *Sargassum*, which has not been previously reported, is very close to that of seawater. This is consistent with its relatively slow rate of rise through the water column, and its ability to be mixed to depth during wind events (Johnson & Richardson, 1977; Woodcock, 1993). The size of *Sargassum* rafts can vary considerably, from just a few centimeters for a small individual plant to aggregations spanning kilometers (Gower et al., 2006; Lapointe, 1995; Parr, 1939; Schell et al., 2015; Stoner, 1983). However, here we find the effective radius of the rafts is on the order of 90 cm. While *Sargassum* observations have been seen as qualitatively consistent with the theory governing inertial particles (Beron-Vera et al., 2015), no validation for effective radius of *Sargassum* aggregations has previously been reported.

The measurements in this study give the first comprehensive indication of whether *Sargassum* rafts are deflected due to inertia when encountering eddies or other sources of acceleration. The equations for these inertial interactions have been described for spherical particles (Beron-Vera et al., 2015; Maxey & Riley, 1983), but this technique for estimating an effective radius could be useful for improving existing models of nonspherical, nonuniform floating objects such as *Sargassum* (Brooks et al., 2018; Franks et al., 2016; Putman et al., 2018) or floating debris (Lebreton et al., 2012). The methods used here could also potentially be used to discriminate between *Sargassum* and other floating algae detected using AFAI such as *Trichodesmium*, which should have very different inertial responses.

Several of the major pathways of *Sargassum* transport are characterized by high eddy activity, such as the Gulf Stream and the North Brazil Current. (Coles et al., 2013; Putman et al., 2018). Inertial forces tend to favor entrainment of *Sargassum* in cyclonic eddies, and we found that inertia caused *Sargassum* to become entrained in eddies five times more frequently than noninertial particles. Eddies can impact growth by locally raising or lowering the depth of the thermocline, as well as through localized strong vertical velocities (e.g Falkowski et al., 1991; Lévy et al., 1998; Martin & Richards, 2001), and cause changes in food web structure and consumer growth rates (Shulzitski et al., 2015; Wells et al., 2017). We hypothesize that *Sargassum* entrained in cyclonic eddies may experience increased access to nutrients both directly from upwelling and potentially recycled from fish excretion (Lapointe et al., 2014) and retained by the eddy structure and shoaled thermocline.

In addition to changing the local environmental conditions associated with eddies, inertial effects also alter the trajectories of *Sargassum* rafts. Incorporation into cyclonic eddies will tend to advect Sargassum to the northwest in this region. The modeled increase in retention in the Gulf of Mexico may help maintain the putative seed population there (Brooks et al., 2018). The increase in connectivity from the Sargasso Sea southward into the tropics provides a mechanism for replenishment of the population that most directly influences the Caribbean (Brooks et al., 2018; Franks et al., 2016; Putman et al., 2018). Changes in eddy dynamics and frequency, particularly during spring and summer *Sargassum* growing seasons, could thus influence variability in *Sargassum* washups in the Caribbean.

The estimates of inertial effects in this study assume *Sargassum* has a constant density and effective radius. However, *Sargassum* buoyancy changes as it ages due to colonization by epiflora and epifauna, and loss of structural integrity of gas-filled pneumatocysts (Johnson & Richardson, 1977). This implies that the influence of inertia is likely to vary seasonally as *Sargassum* ages. Inertial effects should be more pronounced in the spring and summer when production of new *Sargassum* biomass is high. Because of this age effect, estimates in this study of *Sargassum* escaping the subtropical gyre may be an upper bound. Given that the gyre accumulates *Sargassum* over long timescales, there is likely to be a substantial population of older biomass there (Brooks et al., 2018), which would at least partially offset the increased inertial effects due to higher latitude. Wind influence on raft size distribution could also lead to spatial differences in inertial effects.

Inertial effects may be important for efforts aimed at predicting *Sargassum* beaching events such as the Sargassum Early Advisory System (Webster & Linton, 2013) and the Sargassum Watch System (Maréchal et al., 2017). The difference between inertial particles and a traditional particle model in these experiments often results in differences of tens of kilometers in projected trajectory over just 1 week. Inertial forces tend to cause more *Sargassum* to enter and be retained in the Caribbean and Gulf of Mexico than noninertial models would predict.

References

Adobe Systems (2011). *Adobe Photoshop CS5 12.1*. San Jose, CA: Adobe Systems Incorporated.

AVISO (2018). Value-added products: Finite size Lyapunov exponents and orientations of associated vectors. Accessed July 11, 2018. www.aviso.altimetry.fr

Beron-Vera, F. J., Olascoaga, M. J., Haller, G., Farazmand, M., Triñanes, J., & Wang, Y. (2015). Dissipative inertial transport patterns near coherent Lagrangian eddies in the ocean. *Chaos*, *25*(8). https://doi.org/10.1063/1.4928693

Beron-Vera, F. J., Olascoaga, M. J., & Lumpkin, R. (2016). Inertia-induced accumulation of flotsam in the subtropical gyres. *Geophysical Research Letters*, *43*, 12,228–12,233. https://doi.org/10.1002/2016GL071443

Brooks, M. T., Coles, V. J., Hood, R. R., & Gower, J. F. R. (2018). Factors controlling the seasonal distribution of pelagic Sargassum. *Marine Ecology Progress Series*, *599*, 1–18. https://doi.org/https://doi.org/10.3354/meps12646

Cartwright, J. H. E., Feudel, U., Károlyi, G., de Moura, A., Piro, O., & Tél, T. (2010). Dynamics of finite-size particles in chaotic fluid flows. In M. Thiel et al. (Eds.), *Nonlinear dynamics and chaos: Advances and perspectives* (pp. 51–87). Springer-Verlag. https://doi.org/10.1007/978-3-642-04629-2

Chassignet, E., Hurlburt, H., Metzger, E. J., Smedstad, O., Cummings, J., Halliwell, G., et al. (2009). US GODAE: Global ocean prediction with the HYbrid Coordinate Ocean Model (HYCOM). *Oceanography*, *22*(2), 64–75. https://doi.org/10.5670/oceanog.2009.39

Coles, V. J., Brooks, M. T., Hopkins, J., Stukel, M. R., Yager, P. L., & Hood, R. R. (2013). The pathways and properties of the Amazon River Plume in the tropical North Atlantic Ocean. *Journal of Geophysical Research: Oceans*, *118*, 6894–6913. https://doi.org/10.1002/2013JC008981

Ocean Color. (2018). National Aeronautics and Space Administration Goddard Space Flight Center. Accessed July 10, 2018. http://oceancolor.gsfc.nasa.gov

d'Ovidio, F., Fernández, V., Hernández-García, E., & López, C. (2004). Mixing structures in the Mediterranean Sea from finite-size Lyapunov exponents. *Geophysical Research Letters*, *31*, L17203. https://doi.org/10.1029/2004GL020328

Early, J. J., Samelson, R. M., & Chelton, D. B. (2011). The evolution and propagation of quasigeostrophic ocean eddies. *Journal of Physical Oceanography*, *41*(8), 1535–1555. https://doi.org/10.1175/2011JPO4601.1

Falkowski, P. G., Ziemann, D., Kolber, Z., & Bienfang, P. K. (1991). Role of eddy pumping in enhancing primary production in the ocean. *Nature*, *352*(6330), 55–58. https://doi.org/10.1038/352055a0

Franks, J. S., Johnson, D. R., & Ko, D. S. (2016). Pelagic Sargassum in the tropical North Atlantic. *Gulf and Caribbean Research*, *27*(1). https://doi.org/10.18785/gcr.2701.08

Franks, J. S., Johnson, D. R., Ko, D. S., Rubio, G. S., Hendon, J. R., & Lay, M. (2011). Unprecedented influx of pelagic Sargassum along Caribbean Island coastlines during summer 2011. *Proceedings of the Gulf and Caribbean Fisheries Institute*, *64*, 6–8.

Garraffo, Z. D., Mariano, A. J., Griffa, A., Veneziani, C., & Chassignet, E. P. (2001). Lagrangian data in a high-resolution numerical simulation of the North Atlantic I. Comparison with in situ drifter data. *Journal of Marine Systems*, *29*(1-4), 157–176. https://doi.org/10.1016/S0924-7963(01)00015-X

Gower, J., Hu, C., Borstad, G., & King, S. (2006). Ocean color satellites show extensive lines of floating Sargassum in the Gulf of Mexico. *IEEE Transactions on Geoscience and Remote Sensing*, *44*(12), 3619–3625. https://doi.org/10.1109/TGRS.2006.882258

Haller, G., & Sapsis, T. (2008). Where do inertial particles go in fluid flows? *Physica D: Nonlinear Phenomena*, *237*(5), 573–583. https://doi.org/10.1016/j.physd.2007.09.027

Hu, C. (2009). A novel ocean color index to detect floating algae in the global oceans. *Remote Sensing of Environment*, *113*(10), 2118–2129. https://doi.org/10.1016/j.rse.2009.05.012

Johnson, D. L., & Richardson, P. L. (1977). On the wind-induced sinking of Sargassum. *Journal of Experimental Marine Biology and Ecology*, *28*(3), 255–267. https://doi.org/10.1016/0022-0981(77)90095-8

Langin, K. (2018). Seaweed masses assault Caribbean islands. *Science*, *360*(6394), 1157–1158. https://doi.org/10.1126/science.360.6394.1157

Lapointe, B. E. (1995). A comparison of nutrient-limited productivity in Sargassum natans from neritic vs. oceanic waters of the western North Atlantic Ocean. *Limnology and Oceanography*, *40*(3), 625–633. https://doi.org/10.4319/lo.1995.40.3.0625

Lapointe, B. E., West, L. E., Sutton, T. T., & Hu, C. (2014). Ryther revisited: Nutrient excretions by fishes enhance productivity of pelagic Sargassum in the western North Atlantic Ocean. *Journal of Experimental Marine Biology and Ecology*, *458*, 46–56. https://doi.org/10.1016/j.jembe.2014.05.002

Lebreton, L. C. M., Greer, S. D., & Borrero, J. C. (2012). Numerical modelling of floating debris in the world's oceans. *Marine Pollution Bulletin*, *64*(3), 653–661. https://doi.org/10.1016/j.marpolbul.2011.10.027

Lévy, M., Mémery, L., & Madec, G. (1998). The onset of a bloom after deep winter convection in the northwestern Mediterranean Sea: Mesoscale process study with a primitive equation model. *Journal of Marine Systems*, *16*(1–2), 7–21. https://doi.org/10.1016/S0924-7963(97)00097-3

Maréchal, J. P., Hellio, C., & Hu, C. (2017). A simple, fast, and reliable method to predict Sargassum washing ashore in the Lesser Antilles. *Remote Sensing Applications: Society and Environment*, *5*(May 2016), 54–63. https://doi.org/10.1016/j.rsase.2017.01.001

Martin, A. P., & Richards, K. J. (2001). Mechanisms for vertical nutrient transport within a North Atlantic mesoscale eddy. *Deep-Sea Research Part II: Topical Studies in Oceanography*, *48*(4–5), 757–773. https://doi.org/10.1016/S0967-0645(00)00096-5

Maxey, M. R., & Riley, J. J. (1983). Equation of motion for a small rigid sphere in a nonuniform flow. *Physics of Fluids*, *26*(4), 883–889. https://doi.org/10.1063/1.864230

Morrow, R., Birol, F., Griffin, D., & Sudre, J. (2004). Divergent pathways of cyclonic and anti-cyclonic ocean eddies. *Geophysical Research Letters*, *31*, L24311. https://doi.org/10.1029/2004GL020974

Parr, A. E. (1939). Quantitative observations on the pelagic Sargassum vegetation of the western North Atlantic. *Bulletin of the Bingham Oceanography Collection*, *6*, 1–94.

Putman, N. F., Goni, G. J., Gramer, L. J., Hu, C., Johns, E. M., Trinanes, J., & Wang, M. (2018). Simulating transport pathways of pelagic Sargassum from the equatorial Atlantic into the Caribbean Sea. *Progress in Oceanography*, *165*, 205–214. https://doi.org/10.1016/j.pocean.2018.06.009

R Core Team (2018). *R: A language and environment for statistical computing*. Vienna, Austria: R Foundation for Statistical Computing. https://www.R-project.org

SaWS (2018). University of South Florida satellite-based *Sargassum* watch system. Accessed July 10, 2018. Retrieved from https://optics.marine.usf.edu/projects. SaWS.html

Schell, J. M., Goodwin, D. S., & Siuda, A. N. S. (2015). Recent Sargassum inundation events in the Caribbean: Shipboard observations reveal dominance of a previously rare form. *Oceanography*, *28*(3), 8–10. https://doi.org/https://doi.org/10.5670/oceanog.2015.70

Shulzitski, K., Sponaugle, S., Hauff, M., Walter, K., D'Alessandro, E. K., & Cowen, R. K. (2015). Close encounters with eddies: Oceanographic features increase growth of larval reef fishes during their journey to the reef. *Biology Letters*, *11*(1), 20140746. https://doi.org/10.1098/rsbl.2014.0746

Smetacek, V., & Zingone, A. (2013). Green and golden seaweed tides on the rise. *Nature*, *504*(7478), 84–88. https://doi.org/10.1038/nature12860

Stoner, A. W. (1983). Pelagic Sargassum: Evidence for a major decrease in biomass. *Deep Sea Research Part A. Oceanographic Research Papers*, *30*(4), 469–474. https://doi.org/10.1016/0198-0149(83)90079-1

Wang, M., & Hu, C. (2018). On the continuity of quantifying floating algae of the Central West Atlantic between MODIS and VIIRS. *International Journal of Remote Sensing*, *39*(12), 3852–3869. https://doi.org/10.1080/01431161.2018.1447161

Wang, M., Hu, C., Cannizzaro, J., English, D., Han, X., Naar, D., et al. (2018). Remote sensing of *Sargassum* biomass, nutrients, and pigments. *Geophysical Research Letters*, *45*, 12,359–12,367. https://doi.org/10.1029/2018GL078858

Webster, R. K., & Linton, T. (2013). Development and implementation of Sargassum Early Advisory System (SEAS). *Shore & Beach*, *81*(3), 1–6.

Wells, R. J. D., Rooker, J. R., Quigg, A., & Wissel, B. (2017). Influence of mesoscale oceanographic features on pelagic food webs in the Gulf of Mexico. *Marine Biology*, *164*(4), 1–11. https://doi.org/10.1007/s00227-017-3122-0

Woodcock, A. H. (1993). Winds subsurface pelagic Sargassum and Langmuir circulations. *Journal of Experimental Marine Biology and Ecology*, *170*(1), 117–125. https://doi.org/10.1016/0022-0981(93)90132-8